Charge injection across a polymeric heterojunction

van Woudenbergh, T; Wildeman, J; Blom, PWM

Published in:
Physical Review. B: Condensed Matter and Materials Physics

DOI:
10.1103/PhysRevB.71.205216

Publication date:
2005

Charge injection across a polymeric heterojunction

T. van Woudenbergh, J. Wildeman, and P. W. M. Blom*
Materials Science Centre, University of Groningen, Nijenborgh 4, NL-9747 AG Groningen, The Netherlands
(Received 24 August 2004; revised manuscript received 13 October 2004; published 31 May 2005)

The charge injection across a polymeric heterojunction of a poly-p-phenylene vinylene derivative (injecting layer) and poly(9,9-dioctylfluorene) (accepting layer) is investigated. The electric field in the accepting layer is obtained after correcting the applied voltage for the voltage drop across the injecting layer due to the buildup of space charge. At high electric fields, the current across the polymeric heterojunction exhibits only a weak dependence on the field due to the absence of image force effects, in agreement with model predictions. The strong dependence at low fields can be explained by taking the increase of the Fermi level into account, which effectively modifies the barrier for charge carriers waiting for a jump across the heterojunction.

DOI: 10.1103/PhysRevB.71.205216 PACS number(s): 72.80.Le, 73.61.Ph, 85.60.Jb

I. INTRODUCTION

A typical polymeric light-emitting diode (PLED) consists of a thin layer of undoped conjugated polymer sandwiched between two electrodes. Experimentally, attention has especially been focused on PLEDs that contain the conjugated polymer poly(phenylene vinylene) (PPV) or its derivatives which have an external conversion efficiency larger than 1% photons/charge carrier.[1] The electron conduction in the PPV derivatives proved smaller than the hole conduction, which was attributed to the presence of traps[2] or lower electron mobility.[3] For PLEDs, in which both electrons and holes are injected, the different conduction of electrons and holes is directly responsible for the distribution of the light output in the polymer layer. Model calculations of a PLED with Ohmic contacts showed that the light output is mainly confined in a region close to the cathode, due to the reduced electron conduction.[2] As a result, nonradiative energy transfer to the metallic cathode strongly reduces the quantum efficiency (photon/charge carrier) of the PLED at low voltages.

The use of heterojunctions has proven to be very useful, as has been demonstrated in light-emitting diodes (LEDs) based on evaporated small molecules [organic LEDs (OLEDs)]. In these multilayer OLEDs, the active part consists of various layers with various functions, leading to highly efficient devices.[4] These layers are chosen to have properties, such as hole and electron transport, hole or electron blockage, and high emission. For PLEDs, the preparation of multilayers from a solution is more problematic because the bottom layer can be dissolved during the application of a subsequent layer. The optoelectronic properties of organic multilayer devices are strongly dependent on the offset in band-edge positions. For example, the presence of a large energy barrier at an interface blocks highly mobile charge carriers and prevents radiative losses near the metal electrodes.

Recently, a theoretical model describing charge transport across an interface from one organic dielectric into another was developed by Arkhipov *et al.*[5] So far, no systematic experimental study has been conducted to investigate the charge transport across organic-organic interfaces (OOIs). Attention has mainly been focused on the injection of charges from a metallic electrode into an organic dielectric. For inorganic semiconductors, the charge injection is described by thermionic emission and tunneling.[6] For organic semiconductors on the other hand, the charge injection is governed by the hopping of charge carriers into localized sites that are energetically disordered.[7] This energetic disorder is caused by fluctuations in the energy of the localized transport sites, described by a Gaussian density of states (DOS) with a width σ of typically 0.1 eV.[8] The presence of energetic disorder is expected to strongly reduce the temperature dependence of the charge injection process, as has been experimentally confirmed by studies on PPV.[9] A fundamental difference between charge transport across an organic-organic interface (OOI) and a metal-organic interface (MOI) is that for an MOI the image charge potential causes a barrier lowering, which strongly influences the field dependence of the charge injection.[7] For an OOI, low carrier concentrations and slow dielectric relaxation in the "electrode" (injecting layer) do not allow the creation of an image charge, and the image potential is absent. Therefore, it is expected that the charge transport across an OOI is only weakly field dependent as compared to the MOI.[5]

In the present study, the charge injection across a polymeric heterojunction is investigated. The heterojunction is formed by a PPV hole injecting layer with a poly (9,9-dioctylfluorene) (PFO) hole accepting layer on top. For such a system, an interface energy barrier for hole transport is formed between the PPV and the PFO due to the offset between the highest occupied molecular orbits (HOMOs) of both polymers (inset Fig. 1). PPV has a HOMO of 5.3 eV,[10] while for PFO the HOMO is about 5.8 eV,[11] resulting in an interface energy barrier of $\phi_B \sim 0.5$ eV. It is demonstrated that such a large injection barrier strongly limits the hole current across the heterojunction. At high applied voltages, the weak field dependence of the current across the polymeric heterojunction is in agreement with the predictions of the model from Arkhipov *et al.*[5] At low fields, the experimental current shows a stronger field dependence as compared to the model. This is attributed to a change of the effective barrier height due to the filling of states at the injecting interface.

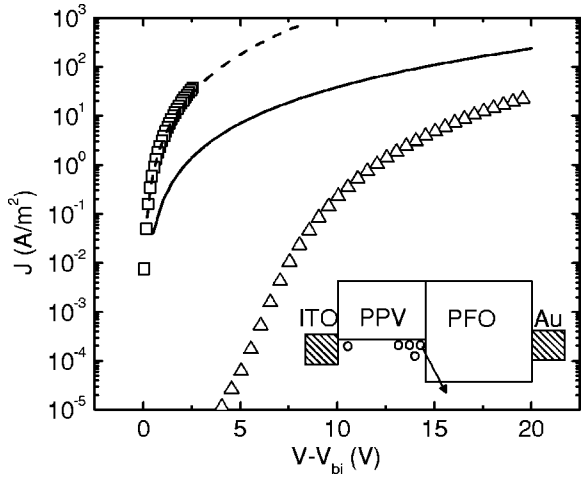

FIG. 1. Current density as a function of voltage for an ITO/PPV/Au hole-only device ($d=140$ nm) (squares) together with an ITO/PPV/PFO/Au double-layer device ($d=140+230$ nm) (triangles). The dashed line is the calculated SCLC through the single-layer device, the solid line depicts the calculated SCLC through the double layer in the absence of an interface barrier. The inset shows the schematic energy band diagram of the double-layer device.

II. EXPERIMENT

The two-layer devices consist of an indium tin oxide (ITO) bottom electrode, covered with a layer of a bi-ethyl hexyl-PPV (BEH-PPV) derivative, that has been spin coated from chloroform (6 mg/ml). The top layer consists of PFO, that has been spin coated from toluene (20 mg/ml). The BEH-PPV derivative is not soluble in toluene. Via thickness measurements, it has been confirmed that the thickness of the two-layer devices equals the thickness of two separate layers (PPV and PFO), prepared with the same spin-coat conditions. Two batches have been used. For one, the bottom layer is $d_{\mathrm{PPV}}=100$ nm, with a top layer of $d_{\mathrm{PFO}}=70$ nm, the other batch has a bottom layer $d_{\mathrm{PPV}}=140$ nm ($d_{\mathrm{PFO}}=100$, 140, and 230 nm). On top of the PFO, a Au contact has been evaporated. For such a device (inset Fig. 1), the bottom ITO electrode forms an Ohmic contact on PPV, while the Au top contact blocks electron injection into the PFO layer, and the current throughout the device is carried by holes (hole only device). As a reference, single layer hole only devices have been made, where the ITO bottom electrode has been covered with the BEH-PPV derivative, and on top a Au electrode has been evaporated.

III. RESULTS

A. Injection-limited transport across the polymeric heterojunction

In Fig. 1, the current-density voltage (J-V) characteristic of a PPV/PFO double-layer device is shown. The thicknesses amount to 140 nm and 230 nm for the PPV and PFO, respectively. It is observed that the current of the two-layer PPV/PFO devices is indeed strongly reduced with respect to the PPV single-layer device. The dashed line is the space-charge limited (SCL) hole current calculated with a field-dependent mobility of the form $\mu_h(E)=\mu_h(0)\exp(\gamma\sqrt{E})$. A zero-field mobility $\mu_h(0)$ of 1.5×10^{-10} m^2/V s and a field activation factor γ of 3×10^{-4} (m/V)$^{1/2}$ have been obtained. As a reference also, the maximum attainable current for the double-layer device is calculated: This current is reached when the OOI energy barrier is not present and the current is only limited by the buildup of space charge in the two layers. The solid line shows the calculated space SCL current (SCLC) for the two-layer device. For the mobility of PFO, $\mu_h(0)=1\times10^{-9}$ m^2/V s and $\gamma=5\times10^{-5}$ (m/V)$^{1/2}$ have been used.[11,12]

It is observed that at low voltages, the measured current density for the two-layer device (triangles) is more than three orders of magnitude lower than the calculated bulk SCLC (solid line), which indicates that the current across the heterojunction is indeed strongly injection limited. From this observation it is expected that the field distribution across the PFO layer is uniform, since the amount of charge carriers entering the PFO is too small to locally change the field. It should be noted that this constant electric field in the accepting PFO layer, E_{PFO}, determines the charge transport across the heterojunction interface.[5] In order to analyze this dependence of the injection-limited current (ILC) on the field across the PFO, the applied voltage needs to be corrected for the voltage drop across the bottom PPV layer. For very thin top PFO layers, an eventual voltage drop across the bottom PPV injecting layer can have a relatively large influence on the electrical characteristics. It is important to realize that the charge transport through the PPV-based injecting layer is SCL. As a result, this layer only becomes conductive when charge is injected into it. Since this charge is not neutralized, it will lead to a buildup of electric field in the PPV, and subsequently to a substantial voltage drop across this layer.

B. Potential drop across the PPV injecting layer

For SCL transport, the current is proportional to the total amount of injected charges, which makes it possible to decouple the hole transport in the PPV and the transport across the heterojunction. In case of a field-independent mobility, the voltage drop across the PPV (V_{PPV}) for a given current-density J of the double-layer device is simply given by (ϵ=the dielectric permittivity)

$$V_{\mathrm{PPV}}^2=\frac{Jd_{\mathrm{PPV}}^3}{9/8\epsilon\mu}. \tag{1}$$

As an example, for a current density of $J=10$ A/m^2, a thickness of $d_{\mathrm{PPV}}=140$ nm for the PPV bottom layer, and a mobility of $\mu_h(0)=1.5\times10^{-10}$ m^2/V s, the voltage drop over the PPV layer is about 2.5 V, while the experimental voltage drop over the total device is about 9 V for a PFO thickness of $d_{\mathrm{PFO}}=100$ nm to 18 V for $d_{\mathrm{PFO}}=230$ nm. As a result for a thin PFO top layer (100 nm), this 2.5 V amounts to almost one-third of the total voltage drop. In the case of a field-dependent mobility, the voltage drop can be solved numerically from the one-carrier SCLC model.[2] It should be noted that such a procedure correctly provides the voltage drop across the PPV layer of the heterojunction device, since both

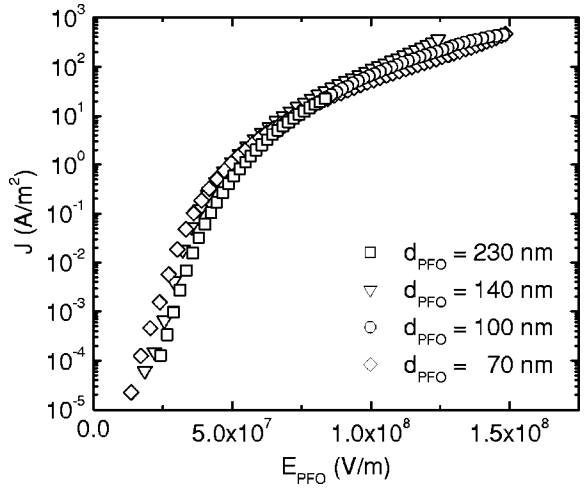

FIG. 2. Current density (J) versus the electric field E_{PFO} in the accepting layer, with the applied voltage being corrected for the voltage drop across the PPV bottom layer. One double-layer device consists of a PPV bottom layer with $d_{\mathrm{PPV}}=100$ nm and a top PFO layer of $d_{\mathrm{PFO}}=70$ nm, the other devices have a PPV bottom layer of $d_{\mathrm{PPV}}=140$ nm and top PFO layers of $d_{\mathrm{PFO}}=100$, 140, and 230 nm, respectively.

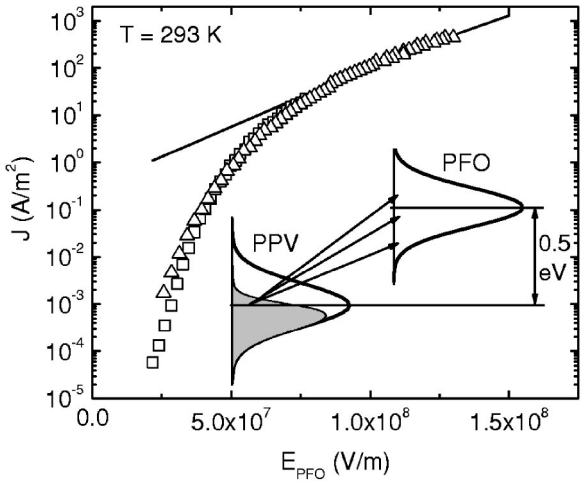

FIG. 3. $J-E_{\mathrm{PFO}}$ characteristic for $d_{\mathrm{PFO}}=230$ nm (squares) and $d_{\mathrm{PFO}}=70$ nm (triangles) device at room temperature, together with the calculated injection current from the OOI model (solid line). The inset shows the half filled DOS of the PPV at the heterojunction interface, the charge carriers jump from the center of the Gaussian into the states of the PFO, as assumed in the OOI model.[5]

current and voltage drop are related to the total amount of charge inside the layer. However, the field- and carrier density distribution of the single carrier SCLC model are not applicable to the heterojunction device; in the heterojunction device, there will be a large buildup of charge carriers at the blocking junction, as will be later discussed in the device model for the double-layer device. With V_{PPV} known, the voltage drop and field across the PFO layer follows directly from

$$V_{\mathrm{PFO}} = V - V_{\mathrm{PPV}}. \tag{2}$$

The electric field, E_{PFO}, in the PFO top layer now becomes $E_{\mathrm{PFO}}=V_{\mathrm{PFO}}/d_{\mathrm{PFO}}$. Figure 2 shows the resulting $J-E_{\mathrm{PFO}}$ plots for the various double-layer devices. It is observed that J scales with E_{PFO}, as expected for an injection-limited device. Thus, Fig. 2 represents the $J-E_{\mathrm{PFO}}$ relation of the experimental ILC across the PPV-PFO heterojunction.

C. Comparison of the experiment with the OOI model

In the next step, the injection current from PPV into PFO has been compared with the injection model for organic heterointerfaces (OOI model).[5] In this model, the current across a heterojunction from one organic dielectric into another is given by

$$j \propto \int_a^\infty dx \exp(-2kx) \int_{-\infty}^\infty d\varepsilon \mathrm{Bol}(\phi_b + \varepsilon - eE_{\mathrm{PFO}}x) \times g(\varepsilon) w_{\mathrm{esc}}(\varepsilon), \tag{3}$$

where k is the inverse localization radius, ε is the energy, $\mathrm{Bol}(\varepsilon)$ is the energy dependence of the jump rate, $g(\varepsilon)$ is the Gaussian DOS, and $w_{\mathrm{esc}}(\varepsilon)$ is the escape probability. As an input, the energy distribution width σ_{PFO} and the nearest-neighbor distance a_{PFO} in the accepting layer should be known. The width of the distribution, σ_{PFO}, has been taken from time-of-flight measurements on PFO, $\sigma_{\mathrm{PFO}}=0.1$ eV.[13] The nearest-neighbor distance a_{PFO} can be estimated from the length of a PFO monomer, $a_{\mathrm{PFO}}\sim 1$ nm. Furthermore, the barrier height amounts to $\phi_b \sim 0.5$ eV. An inverse localization radius k of 5×10^9 m^{-1} has been used.[14]

As shown in the inset of Fig. 3 in the theoretical model, it is assumed that the DOS at the PPV interface is filled up to the center of the Gaussian distribution, and the charge carriers therefore jump from the maximum of the Gaussian DOS.[5] Using these parameters, the injection current across the OOI can directly be calculated. In Fig. 3, the injection current calculated from the OOI model is plotted together with the experimental $J-E_{\mathrm{PFO}}$ characteristics for $T=293$ K. At higher electric fields ($\sim 10^8$ V/m), the experiment is well described by the OOI model. The calculated injection current from the OOI model in this field range is only weakly field dependent. For comparison, in Fig. 4, the current across the polymeric heterojunction is plotted together with the ILC from a Pt bottom electrode into the PFO layer. For the freshly evaporated Pt, we measured a work function of ~ 5.0 eV in nitrogen atmosphere. This leads to a hole injection barrier of about $\sim 0.8-0.9$ eV, also resulting in a strongly ILC. The ILC from the metallic electrode is modeled with the hopping-based injection model.[7] As expected, the absence of image force lowering in the organic-organic heterojunction leads to a strong reduction of the field dependence as compared to the injection from a metallic electrode.[5]

At low fields, there is a large discrepancy between the experimental current and the OOI model. In the model, it is assumed that the starting energy for a carrier jump across the OOI is the middle of the Gaussian DOS of the injection layer. However, for an organic heterojunction between two

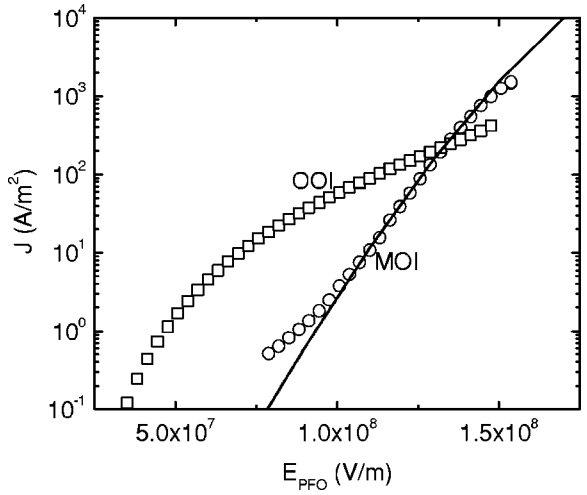

FIG. 4. The ILC across a PPV/PFO interface (OOI, squares) together with the injection current from a Pt anode into PFO (circles). The measurement of the heterojunction is corrected for the voltage drop across the PPV layer. The solid line is a calculation of the injection current for a MOI with $\phi_b = 0.9$ eV.

disordered materials, this starting energy is not a well-defined value, as will be discussed in the next section.

IV. DISCUSSION

A. Low electric field: Influence of charge carrier concentration

For injection of charges from a metal contact into an organic dielectric, the starting point for a charge carrier jump is always the metal Fermi level, independent of the injection current density. However, for an organic heterojunction, the Fermi level—from where a charge carrier is injected—does depend on the injection current because the charge carrier concentration at the interface changes with current, as indicated in the inset of Fig. 7. In a disordered semiconductor, the charge carrier mean energy is at σ^2/kT below the center of the Gaussian DOS for low carrier concentrations,[8] with σ as the width of the energy distribution of the transport sites. This mean energy is then the starting point for the injection of charges across the heterojunction. However, with increasing carrier concentration, the Fermi level passes the equilibration energy, $\varepsilon_F > -\sigma^2/kT$, and the energy level from which the charge carriers are injected now rises with ε_F. Assuming thermal equilibrium, the Fermi level is found from:

$$p = \frac{N_{\text{sites}}}{\sqrt{2\pi}\sigma}\int_{-\infty}^{\infty} d\varepsilon \frac{\exp\left(-1/2\left(\frac{\varepsilon}{\sigma}\right)^2\right)}{1+\exp\left(\frac{\varepsilon-\varepsilon_F}{kT}\right)}, \tag{4}$$

where N_{sites} is the concentration of localized sites in the PPV. In the original OOI model,[5] two situations have been described: One for a half-filled DOS where the injection energy level equals the center of the Gaussian distribution ($\varepsilon_{\text{inj}}=0$), and one for very low carrier densities, where the injection energy level equals the equilibration energy, $\varepsilon_{\text{inj}} = -\sigma^2/kT$. However, it is also pointed out that the OOI model can be applied to an arbitrary injection energy, which results in an effective barrier height, $\phi_{b,\text{eff}} = \phi_b - \varepsilon_{\text{inj}}$. As described above, the additional injection energy ε_{inj} is given by

$$\varepsilon_{\text{inj}} = \begin{cases} \varepsilon_F, & \varepsilon_F > -\dfrac{\sigma^2}{kT} \\ -\dfrac{\sigma^2}{kT}, & \varepsilon_F < -\dfrac{\sigma^2}{kT}, \end{cases} \tag{5}$$

where ε_F is found from Eq. (4).

B. Drift-diffusion device model

In order to take the filling of interface states into account, the charge carrier density at the heterojunction has to be calculated as a function of the electric field over the PFO top layer (E_{PFO}). For this, a numerical drift-diffusion device model is used.[15] In this drift-diffusion device model, the Poisson equation is self-consistently solved together with the continuity equations (including both drift and diffusion of charge carriers) by using the Gummel iteration technique. The device model has been used as is depicted in Fig. 5(a): For the PPV bottom layer, the hole transport parameters are known from single-layer PPV devices, that show the characteristic SCLC both for room temperature ($T=293$ K, see Fig. 1) as well as for low temperatures, e.g., $T=248$ K and $T=198$ K. The SCLC of the single PPV layer has a strong temperature dependence that originates from the thermal activation of the mobility.[2] The activation energy Δ is $\Delta=0.5$ eV. With the mobility in the PPV known, the concentration throughout this layer in the double-layer device can be calculated for a certain current density. This charge distribution is fixed by the boundary charge densities: At the ITO anode, all the states are filled (Ohmic contact), whereas at the heterojunction the charge density is unknown, and so the interface concentration p_{int} is estimated. Concurrent with the charge distribution, the field distribution and resulting voltage drop are also calculated. As a result, for an estimate of p_{int}, the electric field at the heterojunction interface, $E_{\text{PPV,int}}$, as well as the voltage drop across the PPV layer, V_{PPV}, are also obtained.

As input for the double-layer device model, the measured current density J, together with the applied bias V (corrected for a small built-in voltage) are used. As the device model calculates the voltage drop across the PPV layer, V_{PPV}, the voltage drop across the PFO layer $V_{\text{PFO}} = V - V_{\text{PPV}}$ and thus the electric field, $E_{\text{PFO}} = V_{\text{PFO}}/d_{\text{PFO}}$, are also known. The normal component of the electric displacement is constant across an interface, $\epsilon_{\text{PFO}}E_{\text{PFO}} = \epsilon_{\text{PPV}}E_{\text{PPV}}$. Due to the small difference in dielectric permittivity for polymers ($\epsilon_r \sim 3$), this condition reduces to $E_{\text{PPV,int}} = E_{\text{PFO}}$. Running the device model will return a field, $E_{\text{PPV,int}}$, found from the charge distribution in the PPV, together with a field, E_{PFO}, found from the net voltage across the PFO top layer. The charge concentration p_{int} is adjusted until the condition $E_{\text{PPV,int}} = E_{\text{PFO}}$ is fulfilled. For a larger p_{int}, the charge concentration close to the heterojunction interface is enhanced, resulting in

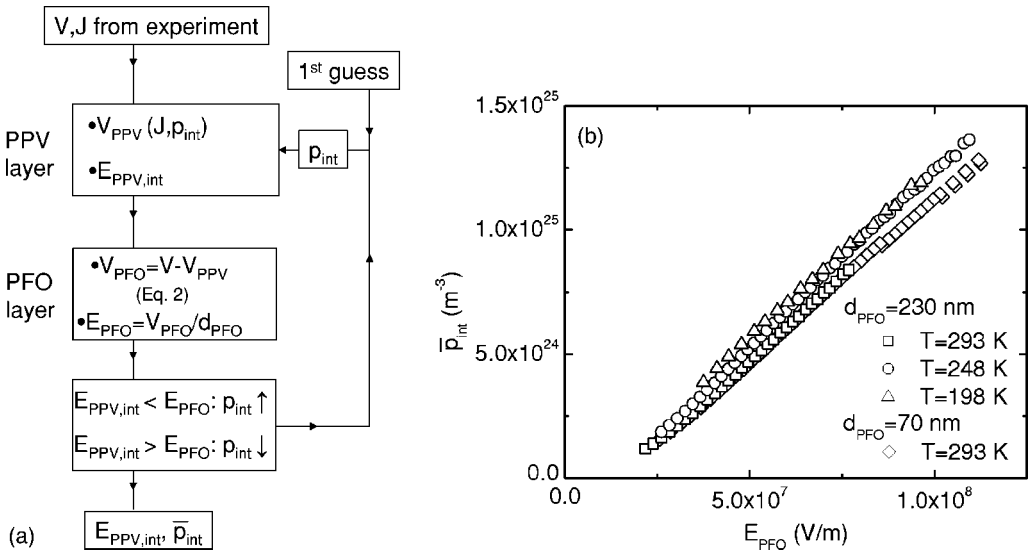

FIG. 5. (a) Flow chart of the operationalization of the drift-diffusion device model: As input, the experimentally measured current density J and bias V are used. An interface concentration p_{int} is estimated, and the voltage drop V_{PPV} and interface field $E_{\mathrm{PPV,int}}$ are calculated. With V_{PPV}, the voltage drop and the electric field across the PFO layer are calculated (second block). Comparing $E_{\mathrm{PPV,int}}$ with E_{PFO} results in a decision for the new value of p_{int} (third block). The calculation is looped until a desired precision in the comparison of $E_{\mathrm{PPV,int}}$ and E_{PFO} is reached. This results in the values of E_{PFO} and $\overline{p_{\mathrm{int}}}$. (b) Spatial averaged charge carrier density $\overline{p_{\mathrm{int}}}$ over the last 1 nm of the PPV at the OOI interface as a function of the electric field in the PFO layer. Different temperatures and device thicknesses are shown as indicated in the label.

a higher $E_{\mathrm{PPV,int}}$. Similarly, a smaller p_{int} results in a lower value of $E_{\mathrm{PPV,int}}$. At the same moment, the field E_{PFO} is rather insensitive to p_{int}. The output of the program is the electric field, E_{PFO}, together with $\overline{p_{\mathrm{int}}}$, the spatial average of the charge concentration over the last monolayer (1 nm). The complete flow diagram used to calculate E_{PFO} and $\overline{p_{\mathrm{int}}}$ from the measured J-V characteristic is shown in Fig. 5(a).

In Fig. 5(b), the calculated charge carrier density $\overline{p_{\mathrm{int}}}$ in the PPV at the PPV/PFO interface is plotted as a function of the electric field in the PFO accepting layer. It is found that the charge concentration ranges from $\overline{p_{\mathrm{int}}} \approx 1.2 \times 10^{24}\ \mathrm{m}^{-3}$ ($\varepsilon_F = -0.32$ eV) at $E_{\mathrm{PFO}} = 2.2 \times 10^7\ \mathrm{V/m}$ up to $\overline{p_{\mathrm{int}}} \approx 1.3 \times 10^{25}\ \mathrm{m}^{-3}$ ($\varepsilon_F = -0.21$ eV) at $E_{\mathrm{PFO}} = 1.1 \times 10^8\ \mathrm{V/m}$, compared with a site density of $N_{\mathrm{sites}} = 3 \times 10^{26}\ \mathrm{m}^{-3}$ for PPV-based polymers.[16] Thus, already at low current densities, there is a substantial filling of the PPV-DOS near the heterojunction interface. In our measurement range, the Fermi level always lies above the equilibration energy, σ^2/kT, and therefore determines the effective energy barrier, $\phi_{b,\mathrm{eff}} = \phi_b - \varepsilon_F$. For $T = 248$ K and $T = 198$ K, roughly the same charge carrier densities $\overline{p_{\mathrm{int}}}$ have been found, as can be seen from Fig. 5(b). The charge carrier density in SCL layers is nearly independent of temperature, since it is governed by electrostatics: Following Poisson's equation, the buildup of the electric field is directly given by the excess charge throughout the device. As a result, the charge carrier density at the interface $\overline{p_{\mathrm{int}}}$ is nearly independent of temperature.

One might argue that jumps from sites deeper into the PPV layer can also contribute to the injection current. However, the band diagrams in Fig. 6 show that the Fermi level is constant over the last few nm in the PPV (constant barrier height), whereas the electronic wave function decays very rapidly ($\sim$0.2 nm) and the charge concentration drops deeper into the PPV. Therefore, the contribution to the injection from deeper lying monolayers decreases very rapidly, and only the last monolayer in the PPV contributes to the injection. Therefore, the average charge concentration in the last monolayer, $\overline{p_{\mathrm{int}}}$, has been chosen to calculate the effective barrier height.

C. Modified organic-organic injection model

Taking this filling of the PPV-DOS at the heterojunction into account, the injection current has been recalculated with

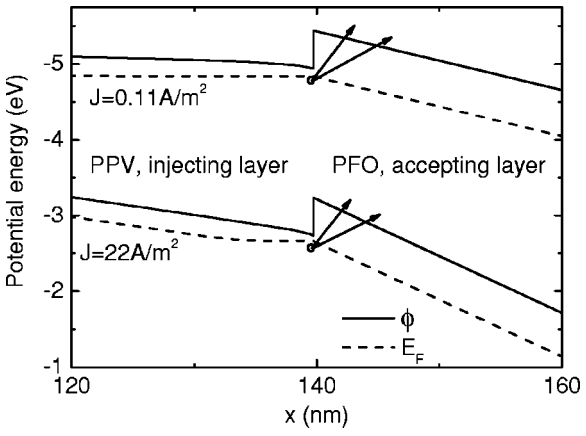

FIG. 6. Band diagram (HOMO, solid line, and hole quasi-Fermi level, dashed line) for two current densities. The area around the PPV/PFO heterointerface is shown. For clarity, the vertical axis is reversed. The work function of the ITO has been taken as a reference ($\phi_{\mathrm{ITO}} = -5.0$ eV).

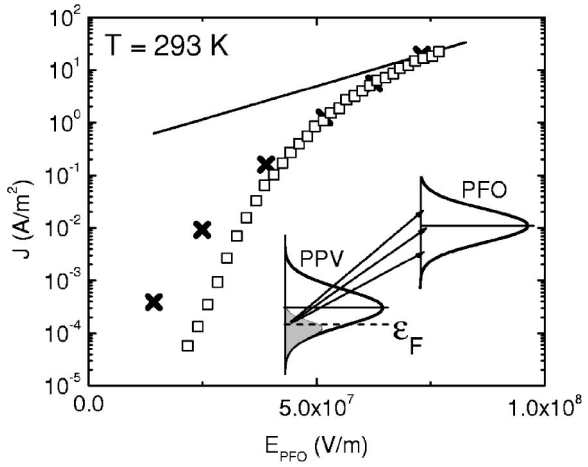

FIG. 7. The measured current across the PPV/PFO heterojunction ($d_{PPV}=140$ nm, $d_{PFO}=230$ nm, squares) together with the calculated ILC over the heterojunction (crosses) for a number of electric fields. This calculation has been performed taking into account the actual Fermi level for each electric field (see inset), due to the filling of the DOS in the PPV near the heterojunction interface. The solid line shows the result from the uncorrected model.

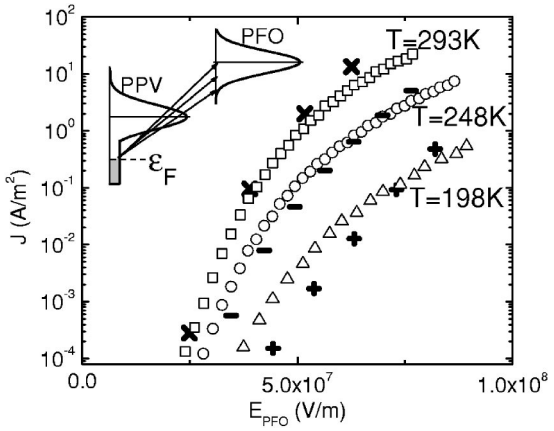

FIG. 8. Experimental characteristics for $T=293$ K (squares), $T=248$ K (circles), and $T=198$ K (triangles) for a ITO/PPV/PFO/Au device with $d_{PPV}=140$ nm and $d_{PFO}=230$ nm, respectively. The symbols $(\times)$, $(-)$, and $(+)$ are the injection currents for this three temperatures as calculated from the corrected OOI model, taking into account a Gaussian DOS together with a uniform trap distribution. The inset shows the modified DOS.

the OOI model. For a given electric field at the heterojunction, the corresponding density at the interface is obtained from Fig. 5(b). Then, from Eq. (4), the position of the Fermi level in the Gaussian is calculated, from which the effective barrier for injection is obtained. This effective barrier is used in the injection model, represented by Eq. (3), to calculate the modified ILC across the OOI. This procedure has been repeated for a number of fields, as shown in Fig. 7 (crosses). For the width σ of the Gaussian DOS of the PPV a value of 0.11 eV has been used.[2]

As shown in Fig. 7, such a correction indeed increases the field dependence of the current across the organic heterojunction at low fields, but is not strong enough to be in agreement with the experimental data. At higher fields, the corrected model exhibits a weak field dependence, similar to the uncorrected model where injection was assumed to start only from the center of the Gaussian DOS. This is because at high fields the Fermi level approaches the center of the Gaussian, and its shift with carrier density will become small due to the large number of available states.

The fact that the corrected model still does not predict the steep field dependence of the experimental current can originate from a number of reasons. First, the shape of the Gaussian at the interface could be different as compared to the bulk value, as suggested by Baldo *et al.*[17] Furthermore, the presence of interface traps could also strongly modify the filling effect at the interface. Measurements on injected-limited PLEDs indicated that interface traps play an important role in the injection process of charge carriers.[18] Typical interface trap densities of $N_{it}=2\times10^{16}$ m^{-2} were found for PPV. As an example, we have assumed a uniform trap distribution with density $H_t=1\times10^{25}$ m^{-3} eV^{-1} for energies -0.6 eV$\leqslant\varepsilon\leqslant0$ eV, as shown in the inset of Fig. 8. This results in an interface trap density of $N_{it}\approx6\times10^{15}$ m^{-2} for a 1 nm thick injection layer, comparable to the interface trap density found for previous experiments.[18] It is observed that the originally Gaussian DOS is modified by a long tail of trap states. The filling of the uniform trap distribution is then responsible for the steep field dependence at low electric field, which weakens when the Fermi level approaches the middle of the Gaussian DOS.

In Fig. 8, the $J-E_{PFO}$ characteristics of the PPV-PFO heterojunction are plotted for $T=293$ K, $T=248$ K, and $T=198$ K. Also shown is the calculated injection current using the modified (Gaussian+uniform trap) DOS. As shown in Fig. 8, the Gaussian DOS, modified by a trap distribution can account for the observed ILC across the PPV/PFO heterojunction.

At higher fields the temperature dependence is in agreement with the model, at low fields the model slightly overestimates the observed temperature dependence. For a better description of the ILC across an organic-organic heterojunction, detailed knowledge about the number and energetic position of the localized interface states is required. For example, extending the temperature range down to nitrogen temperature ($\sim$77 K) would be helpful to say more about the exact DOS but for temperatures lower than 198 K leakage currents start to dominate. The main purpose of this exercise (Fig. 8) is to demonstrate that filling effects at the OOI can completely dominate the observed current across the heterojunction.

V. CONCLUSIONS

It has been demonstrated that a polymeric heterojunction strongly limits the hole current due to an interface energy barrier. In order to obtain the intrinsic field dependence of the ILC across the heterojunction, the potential drop across the injecting layer, due to the buildup of space charge, has to

be taken into account. At high electric fields ($>10^8$ V/m), the observed weak field dependence, due to the absence of image force lowering, is in agreement with the predictions of the OOI model by Arkhipov *et al.*[5] The strong field dependence of the injection current at low fields can be explained by a rapid rise of the Fermi level out of the tail of the PPV DOS, due to the increase in the charge carrier concentration.

ACKNOWLEDGMENTS

The authors would like to thank J. J. A. M. Bastiaansen and Dr. B. M. W. Langeveld-Voss from the TNO Institute of Industrial Technology in Eindhoven for the supply of the PFO. The work of one of the authors (T.v.W.) forms part of the research program of the Dutch Polymer Institute (No. 275).

*Author to whom correspondence should be addressed; electronic mail: p.w.m.blom@phys.rug.nl

[1] J. H. Burroughes, D. D. C. Bradley, A. R. Brown, R. N. Marks, K. Mackay, R. H. Friend, P. L. Burn, A. B. Holmes, Nature (London) **347**, 539 (1990).
[2] P. W. M. Blom and M. C. J. M. Vissenberg, Mater. Sci. Eng., R. **27**, 53 (2000).
[3] L. Bozano, S. A. Carter, J. C. Scott, G. G. Malliaras, and P. J. Brock, Appl. Phys. Lett. **74**, 1132 (1999).
[4] B. W. D'Andrade, M. A. Baldo, C. Adachi, J. Brooks, M. E. Thompson, and S. R. Forrest, Appl. Phys. Lett. **79**, 1045 (2001).
[5] V. I. Arkhipov, E. V. Emelianova, and H. Bässler, J. Appl. Phys. **90**, 2352 (2001).
[6] S. M. Sze, *Physics of Semiconductor Devices*, 2nd ed. (Wiley, New York, 1981).
[7] V. I. Arkhipov, E. V. Emelianova, Y. H. Tak, and H. Bässler, J. Appl. Phys. **84**, 848 (1998).
[8] H. Bässler, Phys. Status Solidi B **175**, 15 (1993).
[9] T. van Woudenbergh, P. W. M. Blom, M. C. J. M. Vissenberg, and J. N. Huiberts, Appl. Phys. Lett. **79**, 1697 (2001).
[10] I. H. Campbell, T. W. Hagler, D. L. Smith, and J. P. Ferraris, Phys. Rev. Lett. **76**, 1900 (1996).
[11] A. J. Campbell, D. D. C. Bradley, and H. Antoniadis, J. Appl. Phys. **89**, 3343 (2001).
[12] T. van Woudenbergh, J. Wildeman, P. W. M. Blom, J. J. A. M. Bastiaansen, and B. M. W. Langeveld-Voss, Adv. Funct. Mater. **14**, 677 (2004).
[13] D. Poplavskyy, T. Kreouzis, A. J. Campbell, J. Nelson, and D. D. C. Bradley, Mater. Res. Soc. Symp. Proc. **725**, 1.4.1 (2002).
[14] E. L. Wolf, *Principles of Electron Tunneling Spectroscopy* (Oxford University Press, New York, 1985).
[15] L. J. A. Koster, E. C. P. Smits, V. D. Mihailetchi, and P. W. M. Blom (unpublished).
[16] C. Tanase, E. J. Meijer, P. W. M. Blom, and D. M. de Leeuw, Phys. Rev. Lett. **91**, 216601 (2003).
[17] M. A. Baldo and S. R. Forrest, Phys. Rev. B **64**, 085201 (2001).
[18] T. van Woudenbergh, P. W. M. Blom, and J. N. Huiberts, Appl. Phys. Lett. **82**, 985 (2003).